

## **DSC AND X-RAY DIFFRACTION STUDY OF POLYMORPHISM IN *n*-ALKYLAMMONIUM CHLORIDES**

*A. Terreros, P. A. Galera-Gómez and E. Lopez-Cabarcos*

Dpto. Química-Física Farmacéutica, Facultad de Farmacia, Universidad Complutense  
28040 Madrid, Spain

### **Abstract**

The influence of the hydrocarbon chain length in the formation of interdigitated and non-interdigitated bilayers in *n*-alkylammonium chlorides has been investigated for chain lengths varying between 8 and 14 carbon atoms. The formation of non-interdigitated bilayers during crystallization from solution is favoured for shorter chains whilst the interdigitated structure is predominant for larger chains. The thermodynamic parameters of the solid to solid phase transitions in the non-interdigitated samples depend on chain length showing the odd-even alternation that characterized homologous series in *n*-paraffins. The solid to liquid crystal phase transition temperatures and enthalpies show a linear dependence with the chain length.

**Keywords:** DSC, polymorphism, X-ray

### **Introduction**

The study of bilayered chain compounds has attracted attention because these systems resemble smectic lipid bilayers. Alkylammonium chlorides, with general formula  $C_nH_{2n+1}NH_3Cl$  (henceforth referred to as  $C_n$ ), crystallize forming bilayers in which they alternate layers of chlorine atoms with layers of alkyl chains [1–8]. The bilayers can be interdigitated or non-interdigitated and the cause of the appearance of one microstructure or the other is not well established and it has been attributed to several factors such as the crystallisation conditions or the type of solvent used [1]. Furthermore, when the bilayers are heated, they exhibit a considerable number of transitions in the solid phase [5] and they also present a liquid crystal phase before the isotropic liquid. In recent years the microstructure of  $C_{10}H_{21}NH_3Cl$  has been studied as a function of temperature and it has been shown [4, 5] that at room temperature the alkyl chains in the C10 bilayer are interdigitated and upon heating they transform to a non-interdigitated arrangement. The decylammonium chloride (C10) has also been used to model the interdigitated to non-interdigitated transition and to construct a Landau theory describing this transition [9].

The existence of various solid phases of the *n*-alkylammonium chlorides has long been established and the transition temperatures and enthalpies reported [10].

However, because the presence of the interdigitated phase is not systematic, the chain length dependence of the thermodynamic parameters has not yet been reported. Although the structure of some *n*-alkylammonium chlorides has been studied using X-ray diffraction [5, 6] and NMR [11] there are still few studies that span a reasonable range of hydrocarbon chain lengths and to our knowledge, the effect of the microstructure on the thermodynamic parameters of the phase transitions has not yet been investigated. The aims of this paper are twofold. The first is to investigate the formation of interdigitated and non-interdigitated bilayers as a function of chain length. The second is to study the influence of the microstructure on the temperature and enthalpy of the solid to solid and solid to liquid-crystal phase transitions. For this purpose we have synthesised samples with chain length varying between 8 and 14 carbon atoms. The study was performed using DSC and X-ray diffraction techniques.

## Experimental

The *n*-alkylamines were purchased from FlukaAG and their purity is all cases higher than 97% (for octylamine and decylamine higher than 99%). The alkylammonium chlorides have been prepared by passing gaseous hydrogen chloride through a solution of the *n*-alkylamine in ether. The resulting precipitate was washed several times with ethyl ether, followed by crystallization from mixed solvents, acetone/ethanol/ethyl-ether, and vacuum dried overnight. The white salts were kept for several months in a dry atmosphere. The DSC measurements were carried out in a Mettler 820 differential scanning calorimeter equipped with a cooler operated by liquid nitrogen. The temperature scale was calibrated using the melting temperatures of indium and zinc. The calibration of the enthalpies was performed using the enthalpy of fusion of indium. The DSC cell was used for heat treating the samples and for calorimetric studies. In each test the sample weighted about 1.5 mg. All samples were heated and cooled in a dry nitrogen gas atmosphere at a rate of 10°C min<sup>-1</sup>. Temperature accuracy is ±0.5°C and accuracy in  $\Delta H$  is around 1% for well-defined peaks. The X-ray diffraction studies were performed using a Philips X'pert PW3050 diffractometer. Silicon powder was used to calibrate the sample to film distance. The diffractograms were recorded covering an angular interval between  $2\theta=1.5$  and  $2\theta=35$  degrees, and using a step size of 0.01 degrees with time per step of 1 second.

## Results and discussion

### *X-ray diffraction*

We have recorded at room temperature the X-ray diffraction patterns of the virgin samples. Even though we have synthesised all the samples following the same procedure the diffraction profiles indicate different microstructures. The diffractograms of C8, C9 and C11 are similar but different from those of C10, C12, C13 and C14. We show in Fig. 1 the diffraction patterns for the samples C8, C9 and C11 and in Fig. 2 the patterns of C10, C12, C13 and C14. The most striking difference between Fig. 1

and Fig. 2 is the presence of a strong reflection in the small angle region for the samples C8, C9 and C11, which has been interpreted as a clear indication of the non-interdigitated bilayer structure. On the contrary, the absence of this peak in C10, C12, C13 and C14 would indicate that these samples develop interdigitated bilayers. A common feature to all the diffraction patterns is that most of the reflections belong to the (001) planes which is characteristic of preferential crystallographic orientation. Crystallographic studies performed by Reynhardt in the C10 indicate that the unit cell is monoclinic for the interdigitated phase and triclinic for the non-interdigitated  $\xi$  phase [5].

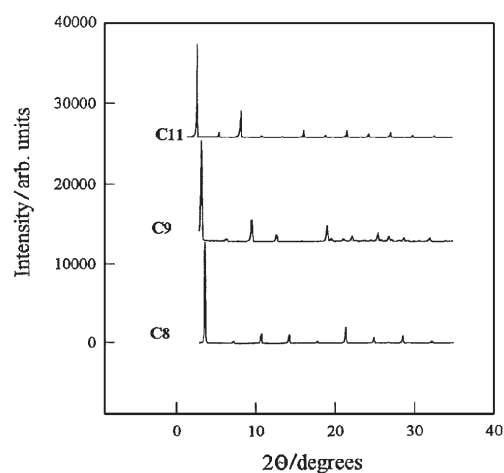


Fig. 1 X-ray diffractograms for *n*-alkylammonium chlorides with  $n_c=8, 9$  and 11

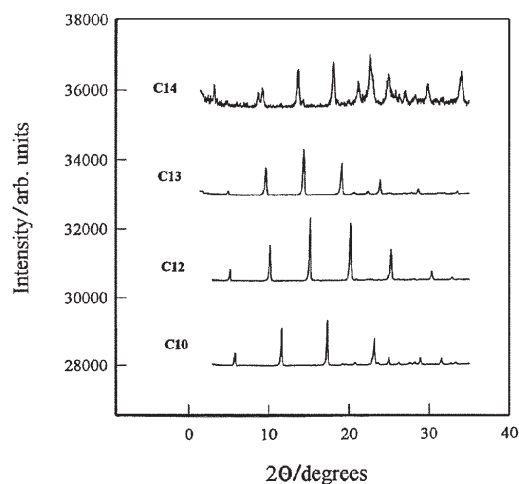
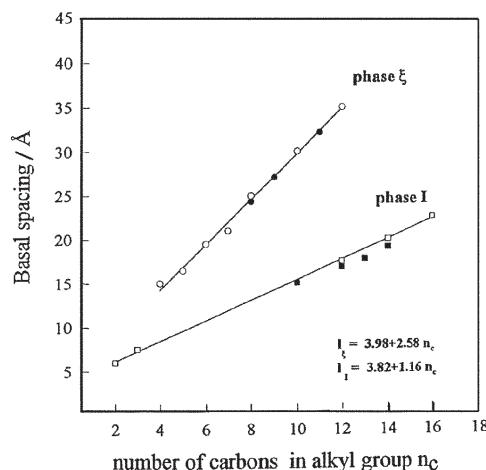


Fig. 2 X-ray diffractograms for *n*-alkylammonium chlorides with  $n_c=10, 12, 13$  and 14



**Fig. 3** The X-ray spacing of the interdigitated and non-interdigitated bilayer as a function of the number of carbon atoms in the chain. The classification of the structure of the surfactants in two types, interdigitated and non-interdigitated, allows to plot following two straight lines the data obtained in the present work (full symbols) together with those collected from literature (open symbols)

The values of the bilayer spacing calculated using the Bragg's equation are shown in Fig. 3. Here we plot the interdigitated and the non-interdigitated bilayer spacings obtained in this work together with others obtained from the literature. In both cases the Bragg's spacing shows a linear dependence with the number of the carbon atoms given by the expressions,

$$l_{\xi}(\text{\AA}) = 3.98 + 2.58n_C \quad (1)$$

$$l_I(\text{\AA}) = 3.82 + 1.16n_C$$

Being  $l_{\xi}$  the spacing of the non-interdigitated phase and  $l_I$  the spacing of the interdigitated one. Both lines span completely the range of carbons in the alkyl group investigated and it seems that the formation of the interdigitated phase is favoured for larger chains. The extrapolation for  $n_C=0$  gives  $l_{\xi}=3.98 \text{ \AA}$  and  $l_I=3.82 \text{ \AA}$  indicating that the inter-layer spacing is slightly larger for the non-interdigitated structure. The length of the full-extended chain as a function of the number of carbons can be calculated using the formula given by Tanford [12]

$$l(\text{\AA}) = 1.5 + 1.265n_C \quad (2)$$

The bilayer thickness of the full-extended chain derived from the above formula is similar to the spacing of the interdigitated bilayer and close to one half of the non-interdigitated one. The linear correlation between basal spacing and chain length points to a structure with the chains near perpendicular to the layer of the polar heads groups.

### Thermal analysis

In the following we study how the microstructure influences the thermodynamic parameters of the phase transitions that appear in samples with different chain lengths. We differentiate between solid to solid and solid to liquid crystal phase transitions.

#### Solid-solid phase transitions

Figure 4 shows the DSC endotherm curves of the virgin samples taken during the heating process from  $-60$  until  $100^{\circ}\text{C}$ . As it occurred with the diffractograms, the DSC curves of the surfactants C8, C9 and C11 are similar and very different from the DSC curves of C11, C12, C13 and C14. We follow the nomenclature introduced by Reynhardt *et al.* [5] to name the phases that appear in the solid state during a heating scan. Thus, for the non-interdigitated samples the first endotherm peak corresponds to the transition from the  $\xi$  phase (triclinic) to the  $\delta$  phase (monoclinic). The second and third peaks correspond to the transitions from  $\delta \rightarrow \beta$  (orthorhombic) and from  $\beta \rightarrow \alpha$  (tetragonal) respectively. The DSC curves of the surfactants C10, C12, C13 and C14 show peculiar features and they are very different from the previous ones. Thus, the DSC curve of C10 presents a broad peak corresponding to transition from the interdigitated I phase (monoclinic) to the  $\alpha$  phase. In the DSC curves of C12, C13 and C14 the transition from the I phase to the  $\alpha$  occurs throughout some intermediate phase, which has not yet been characterised by crystallography.

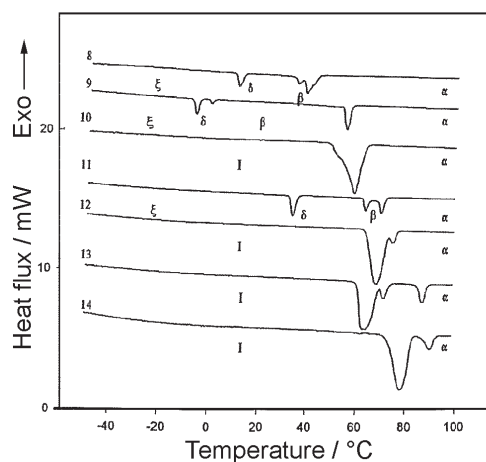


**Fig. 4** DSC curves of the virgin *n*-alkylammonium chloride samples taken during the solid-solid phase transitions. The crystal structure of the solid phases is triclinic  $\xi$ , monoclinic  $\delta$ , orthorhombic  $\beta$  and tetragonal  $\alpha$ . The symbol I corresponds to the monoclinic interdigitated phase

The heated samples were then cooled to  $-60^{\circ}\text{C}$  and heated again from  $-60$  to  $100^{\circ}\text{C}$  to record the DSC curves that are shown in Fig. 5. The DSC curves of the virgin and reheated samples of C8, C9 and C11 are equal whilst for the surfactants C10,

C12, C13 and C14 both curves are different. The total enthalpy of the transitions of the interdigitated virgin samples ( $\Delta H_T$ ) is larger than the equivalent in reheated ones. However, no difference in the enthalpy values was observed between the second and a third heating scans. It seems that independently of  $n_C$ , all the heat-treated samples present non-interdigitated structure and show similar phases and phase transitions. It has been reported [5] that the temperatures and enthalpies of the solid-solid transitions depend upon the thermal history of the samples but our results indicate that they are more dependent on the initial microstructure.

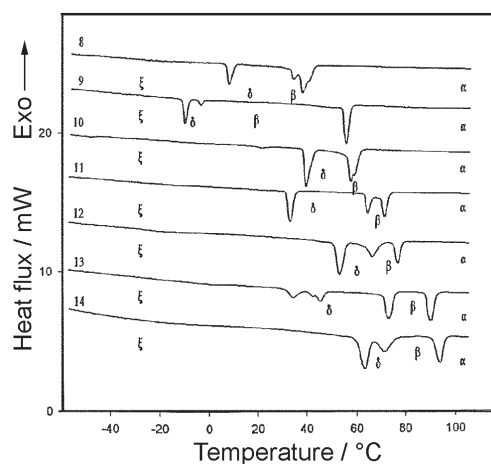
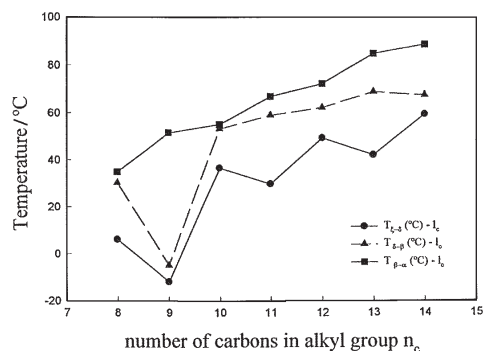


Fig. 5 DSC curves of the heat-treated *n*-alkylammonium crystals

In Table 1 we give the transition temperatures and enthalpies that appear in the non-interdigitated samples. Figure 6 shows the plot of the transition temperatures against the number of carbons in the alkyl group. The odd even effect that has been observed in other surfactant crystals appears for the three transitions. A common behaviour for the curves is that they initially rise and then levels off, the alternation becoming less as the series is ascendant. The odd even effect decreases when the transition temperature increases and also for larger chain lengths. For the transition  $\beta \rightarrow \alpha$  the higher transition temperatures correspond to the odd chains. The alternation of the temperatures has been considered as an effect on the anisotropy of the molecular polarizability arising from increases of chain length on passing from even to odd number of carbons [13, 14]. The increase in flexibility of long chains will progressively decrease the differences in the anisotropies of molecular polarizability between odd and even alkyl derivatives with shorter and more rigid chains. For the transition  $\xi \rightarrow \delta$  the transition temperature is higher when the number of  $\text{CH}_2$  units is even indicating that at lower temperatures the polarizability does not play a decisive role in the transition. In Fig. 7 we show the enthalpy of the solid to solid phase transitions for the heat-treated samples as a function of the chain length. The enthalpy of the  $\xi \rightarrow \delta$



**Fig. 6** Plot of the solid to solid transition temperatures,  $T_{\xi \rightarrow \delta}$ ,  $T_{\delta \rightarrow \beta}$  and  $T_{\beta \rightarrow \alpha}$  vs. the length of the *n*-alkyl chain and  $\delta \rightarrow \beta$  transitions also present the odd-even effect which disappears for the  $\beta \rightarrow \alpha$  transition.

**Table 1** Transition temperatures and enthalpies of the different phases of the *n*-alkylammonium chloride surfactants as a function of the chain length

Phase transition	$\xi \rightarrow \delta$		$\delta \rightarrow \beta$		$\beta \rightarrow \alpha$		$\alpha \rightarrow$ liquid crystal	
	$T/^\circ\text{C}$	$\Delta H/\text{kJ mol}^{-1}$	$T/^\circ\text{C}$	$\Delta H/\text{kJ mol}^{-1}$	$T/^\circ\text{C}$	$\Delta H/\text{kJ mol}^{-1}$	$T/^\circ\text{C}$	$\Delta H/\text{kJ mol}^{-1}$
C8	6.3	2.1	30.4	0.8	35.1	3.4	201.7	6.7
C9	-11.7	2.6	-4.7	0.5	51.7	5.3	195.8	7.0
C10	36.7	4.3	53.4	3.3	55.3	2.2	191.7	7.4
C11	30.0	3.9	59.2	1.8	67.1	2.5	187.1	7.7
C12	49.6	5.5	62.5	3.0	72.4	2.7	182.9	8.1
C13	42.4	4.0	69.1	4.2	85.1	3.9	177.5	8.0
C14	59.7	5.9	67.8	2.7	88.9	4.6	172.7	8.8

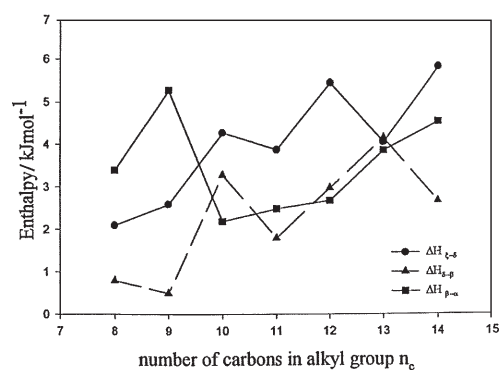


**Fig. 7** Plot of the solid to solid transition enthalpies,  $\Delta H_{\xi \rightarrow \delta}$ ,  $\Delta H_{\delta \rightarrow \beta}$  and  $\Delta H_{\beta \rightarrow \alpha}$  vs. the length of the *n*-alkyl chain

### Solid to liquid crystal phase transition

If we continue heating the samples, we obtain after the solid, the liquid crystal phase before the isotropic liquid. Figure 8 shows the solid to liquid crystal phase transition for the virgin samples as a function of the chain length. The DSC curves of the virgin samples exhibit an exothermic shoulder before the phase transition. The exothermic peak disappears in the heat-treated samples as is shown in Fig. 9 whilst the other features of the DSC curve remain the same. The solid to liquid-crystal phase transition endothermic peak shifts to lower temperatures when the number of carbons in the chain increases. The solidification exothermic peak exhibits the opposite trend and moves to higher temperatures with decreasing the number of carbon atoms in the aliphatic chain.

The temperature of the solid to liquid-crystal transition together with the reverse liquid crystal to solid is plotted in Fig. 10 as a function of the number of carbon atoms

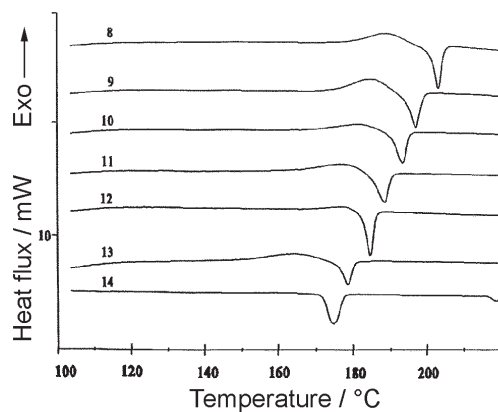


**Fig. 8** DSC curves taken at the solid to liquid-crystal phase transition of virgin samples of *n*-alkylammonium chlorides as a function of the number of carbon atoms in the chain

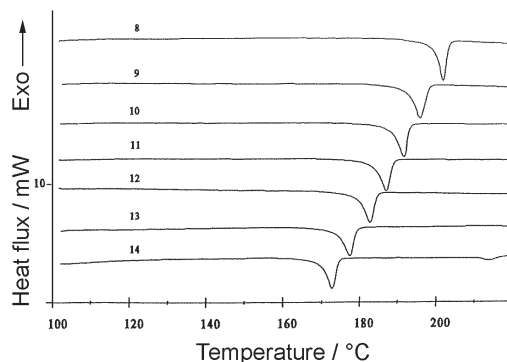


**Fig. 9** DSC curves taken at the solid to liquid-crystal phase transition of the heat-treated samples



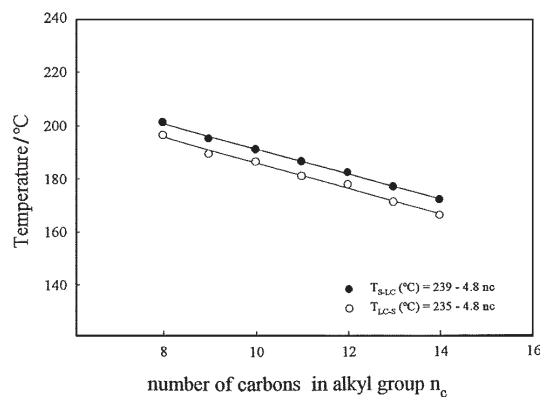


**Fig. 10** Solid to liquid-crystal phase,  $T_{S-LC}$ , and liquid-crystal phase to solid,  $T_{LC-S}$ , transition temperatures as a function of the number of carbon atoms in the alkyl chain

in the chain. In both cases the transition temperature shows a linear dependence with the number of the carbon atoms given by the expressions,

$$\begin{aligned} T_{S-LC} (\text{°C}) &= 239 - 4.8n_c \\ T_{LC-S} (\text{°C}) &= 235 - 4.8n_c \end{aligned} \quad (3)$$

Changing the heating speed from 10 to  $0.5^\circ\text{C min}^{-1}$  the 4 degrees difference in transition temperature on reversing from heating to cooling is reduced to 3 degrees. These seems to indicate that the liquid crystal phase can be supercooled and that the extend of the supercooling is constant throughout the  $n_c$  range considered. The molar enthalpy of the transition, measured in the second heating run, is shown in Fig. 11 and also follows a linear behaviour. Upon cooling the solidification enthalpies follow the opposite trend as is also illustrated in Fig. 11. For a given  $n_c$  the values of both

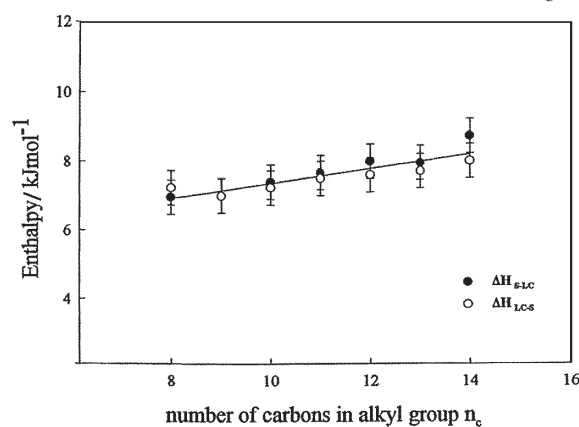


**Fig. 11** Solid to liquid-crystal phase and solidification enthalpies of alkylammonium chlorides as a function of the chain length

enthalpies coincides or at least fall inside the experimental error bar. The dependence of  $\Delta H$  with  $n_C$  is given by,

$$\Delta H = 5.2 + 0.22n_C \quad (4)$$

and seems to indicate a larger degree of chain packing with increasing chain length.

## Conclusions

At room temperature, the microstructure of the virgin samples seems to be dependent on chain length. Shorter chains (C8, C9) favour the non-interdigitated arrangement whereas for larger chains (C10, C12, C13 and C14) the interdigitated bilayer structure is predominant. The solid to solid transitions in the non-interdigitated samples, seems to be independent of the thermal history and if the heating-cooling cycle is repeated no significant change is observed in the transition temperature or in the enthalpy. In the case of interdigitated bilayers the transformation to the non-interdigitated structure is required to observe the solid to solid transitions. Once the transformation has occurred the interdigitated bilayer can not be recovered. The odd-even chain length alternation in melting or crystallization temperatures which is a common phenomena in homologous series and in saturated *n*-paraffins is observed in the solid to solid phase transitions but it did not appear in the solid to liquid crystal transition.

\* \* \*

Grateful acknowledgements are due to DGICYT (Grant N° PB95-0397) and to CICYT (MAT 97-1811E) for the generous support of this investigation.

## References

- 1 A. S. Kertes, H. Gutmann and I. Mayer, *J. Appl. Cryst.*, 4 (1971) 93.
- 2 J. Tsau and D. F. R. Gilson, *Can. J. Chem.*, 52 (1974) 2421.
- 3 J. K. Schenk, G. Chapuis, R. Kind, R. Blinc and J. Selinger, *J. Molec. Struct.*, 176 (1988) 331.
- 4 E. C. Reynhardt, *Chem. Phys. Letters*, 256 (1996) 548.
- 5 E. C. Reynhardt, S. Jurga and K. Jurga, *Mol. Phys.*, 77 (1992) 257.
- 6 J. D. Gault, H. A. Gallardo and H. J. Müller, *Mol. Cryst. Liq. Cryst.*, 130 (1985) 163.
- 7 E. Lopez Cabarcos and P. A. Galera Gomez, *Il Nuovo Cimento*, 16D (1994) 1515.
- 8 E. Sackmann, *Ber. Bunsenges. Phys. Chem.*, 82 (1978) 891.
- 9 R. Kind, R. Blinc, H. Arend, P. Mural, J. Slak, G. Chapuis and J. K. Schenk, *Phys. Rev. A*, 26 (1982) 1816.
- 10 J. Tsau and D. F. R. Gilson, *J. Phys. Chem.*, 72 (1972) 4082.
- 11 J. Tsau and D. F. R. Gilson, *Can. J. Chem.*, 51 (1973) 1990.
- 12 C. Tanford, *J. Phys. Chem.*, 78 (1974) 2469.
- 13 G. W. Gray, 'Advances in Liquid Crystals', Ed. G. H. Brown, Academic Press, New York 1976, Vol. 2, p. 1.
- 14 S. Chandrasekhar, 'Liquid Crystals', Cambridge University Press, Cambridge, London 1980.